DANIEL G. ONDERCIN

THE SPATIAL CHARACTERIZATION OF BIO-OPTICS IN THE SARGASSO SEA

The spatial variability of the bioluminescence and optical properties in the western Sargasso Sea was observed during cruises in August 1986 and March 1988. Measurements of temperature, conductivity, bioluminescence, chlorophyll-*a* fluorescence, and beam attenuation were obtained with a towed paravane undulating over the upper 90 m of the water column. During the spring, 10- to 20-km scales of variability were observed for all parameters. The slopes of the power spectra were between 2 and 3, indicating the dominance of physical processes in defining these length scales. Significant in-phase coherence was observed between chlorophyll fluorescence and beam attenuation, while bioluminescence and temperature showed no coherence with any parameter. During the summer, no significant scales of variability or coherence were observed over an 80-km tow.

INTRODUCTION

The spatial and temporal bioluminescence and optical variability in the Earth's oceans have recently been of great interest to the scientific community. Advances in shipboard and satellite instrumentation have greatly increased our understanding of these properties. In particular, the launching of the Coastal Zone Color Scanner (CZCS)[1] in 1978 has enabled oceanographers to observe the near-surface optical properties on spatial and temporal scales never before realized. The variability of ocean color and how it relates to primary production,[2] chlorophyll concentration,[3] and optical properties[4] have been investigated using the CZCS. Also, the meanders of currents[5] and eddies and how they evolve in time are just a few of the phenomena studied via satellite. Although satellites can observe vast areas of ocean at a glance day after day, they have serious drawbacks. To study the ocean, the satellite must have a cloud-free line of sight, which normally is not a problem in tropical latitudes. But in the more productive northern latitudes, clouds are numerous. Optical properties measured from a satellite can be determined to about one optical depth (about 30 to 35 m in the clearest waters). Additionally, observations can only be made during the day—a time that is limited in the northern latitudes during the winter. Direct measurements of bioluminescence from a satellite are not possible. Relationships must be found that associate the measurements of other bulk properties to bioluminescence.

To supplement the data provided by satellites, APL is developing models to predict the vertical structure of the optical properties in the water column and to extend those predictions in time. The models will enable us to use satellite-observed surface optical properties to produce a vertical profile down to a depth of about 200 m. In the northern latitudes during the winter and when the ocean surface is obscured by clouds, the temporal model will predict the characteristics of the water column from the most recent observations.

To facilitate and validate model development, studies must be undertaken to determine the interaction of phytoplankton (the plant component of plankton) with their physical environment. The optical variability in the upper layers of the oceans is dominated by the processes governing phytoplankton production and their degradation products. The major constituents influencing the optical characteristics of ocean waters are particles that scatter the light and organic pigments (primarily chlorophylls and phaeophytins) that absorb the light. Two instruments have routinely been used recently to continuously monitor particle and chlorophyll concentrations *in situ*: the beam transmissometer and the fluorometer. The beam transmissometer measures the percentage of light received from a collimated beam of light generated 1 m from the detector. Since light attenuates exponentially with depth, the extinction coefficient c (commonly called the beam attenuation coefficient) can be determined by taking the negative natural log of the transmittance T (for a 1-m path length),

$$c = -\ln(T) \; . \qquad (1)$$

The beam attenuation coefficient is linearly related primarily to the scattering of water and particles.[6] Therefore, the transmissometer is an excellent indicator of particle distribution in the water column.

Water color and absorption are related strongly to the diffuse attenuation coefficient K, which is the extinction coefficient for downwelling irradiance. In the open ocean, the dominant absorbers (other than water itself) are primarily chlorophyll found in viable phytoplankton.[7] Chlorophyll concentrations can be estimated to within 20% by measuring phytoplankton's *in situ*

fluorescence with a fluorometer. Relationships have been developed that relate pigment concentrations to K.[8,9]

The main scientific objective of our program has been to acquire a suitable database with which to describe and model the ocean optical variability as a function of pertinent physical and biological processes. To obtain this large synoptic data set of the upper ocean with suitable spatial and temporal resolution, rapid vertical profiling is necessary. We have therefore developed a suite of instruments and platforms that are deployed from a surface vessel. This article will briefly describe the environmental system developed by APL and some results obtained from two cruises in the northern Sargasso Sea, one in August 1986 and the second in late March 1988. The data will contrast the relatively productive waters of the spring cruise to the oligotrophic environment of the midsummer cruise.

MATERIALS AND METHODS

Measuring Systems

APL designed and built an environmental measurement system that characterizes the spatial and temporal structure of the upper ocean.[10] The system comprises three subsystems: a surface mapper, a vertical profiler, and a towed paravane. The surface mapping system (Fig. 1) is designed to be deployed continuously during a cruise through a 60-cm-diameter transducer tube extending about 1 m beneath the ship's hull. The system consists of a bathyphotometer (built at APL to measure the light emitted by bioluminescent organisms), temperature and conductivity sensors, and a Turner Designs fluorometer to measure *in situ* chlorophyll fluorescence. Water is drawn through the bathyphotometer and fluorometer with a well pump. The effluent from the pump is sampled to determine the chlorophyll and phaeophytin concentrations by acetone extraction.

The vertical profiler lowers a suite of instruments to 200 m while the ship is on station. The profiler is a General Oceanics 24-bottle rosette sampler (Fig. 2). Nine bottles have been removed and replaced with a Sea-Bird data acquisition system and a junction box. The instruments mounted on the rosette are Sea-Bird temperature and conductivity sensors; a Parascientific depth transducer; the APL-built bathyphotometer, fluorometer, and blue transmissometer (spectrally filtered at 490 nm); and a Biospherical Instruments K-meter (spectrally filtered at 488 nm). Water samples are obtained with 5-L Niskin bottles to determine nutrient levels and pigment concentrations. Water is drawn through the bathyphotometer and fluorometer and into a net manifold with a submersible pump. The net manifold consists of four 20-μm-mesh nets, which are accessed via remotely controlled solenoid valves. Plankton samples obtained from these nets are analyzed for species identification and enumeration.

The towed paravane system (Fig. 3) is designed to profile rapidly a suite of instruments to a depth of 100 m as the research vessel transits at speeds of 4 to 10 kt. Its payload comprises the same instruments mounted on the rosette, with the exception of the K-meter. The paravane acts much like an airplane in the water. The small vane on the underside of the vehicle moves back and forth, causing it to roll. With a fixed cable length, vehicle roll changes the direction of the wings' dynamic lift, causing the vehicle to rise as it moves perpendicular to the ship's course. The vane angle (and therefore the profiling characteristics of the vehicle) is controlled by a topside HP-9816 computer and a vehicle-mounted microprocessor. The vehicle can be towed at a constant depth, or the depth can be changed over the interval from 10 to 100 m at rates up to 2 m/s.

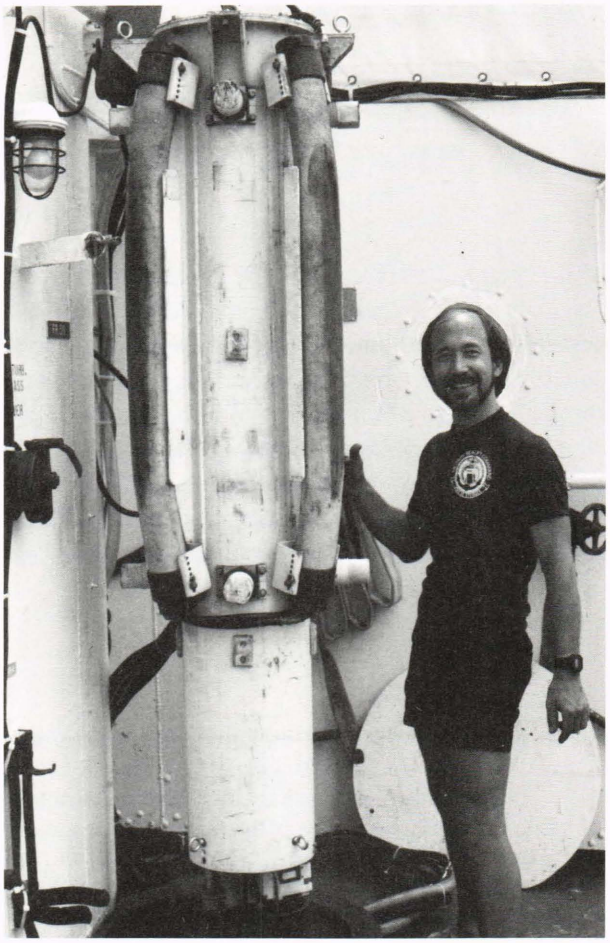

Figure 1—APL's surface mapping system.

The data from either the paravane or the vertical profiler are collected with a Sea-Bird Model SBE-9 underwater unit and an SBE-11 deck unit at a 12-Hz sampling rate. The deck unit transfers the data to the HP-9826 central data-logging computer. The data from the surface mapping system are digitized by an HP-6940 multiprogrammer, which transfers the data to the HP-9826. All data are archived on nine-track tape, with a subset of the data continuously transferred to an HP-9920 "quick-look" computer. This computer displays all data in tabular form and plots and prints select data channels. The data sent to this computer are also stored on nine-track tape, which serves as a backup to the primary system.

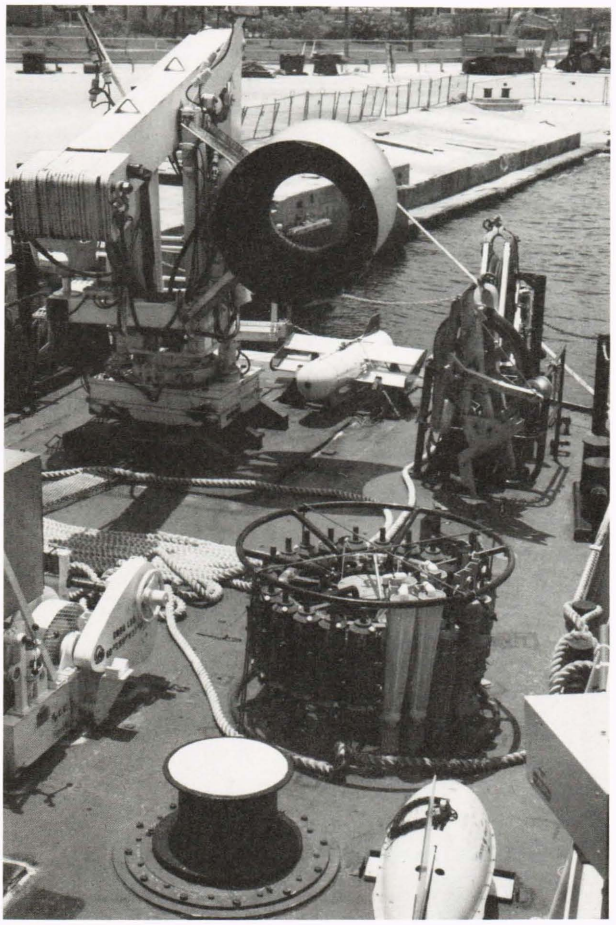

Figure 2—The aft deck of the surface vessel, with the vertical profiler in the foreground.

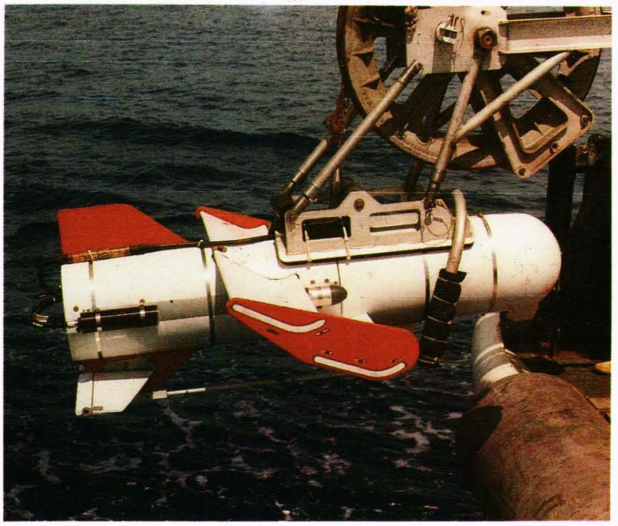

Figure 3—The APL paravane.

Data Processing

All 12-Hz sampling-rate data on the nine-track tapes were averaged to 1-s intervals. Calibration factors were applied and transferred into a database on a VAX-11/750. The processing of a vertical profile cast was split into two sections: the downcast and the upcast. The data from a profiler cast were averaged into 1-m-depth bins, and the resultant profiles were plotted.

The data from a paravane tow were divided into sections, with each section equal to one paravane undulation. These sections were averaged into 1-m-depth bins and stored in an array. Since the paravane tows no shallower than 10 m (for safety reasons), data from the surface mapping system were averaged over the duration of the particular undulation and were entered into the array at 4 m. Data values from 5 to 9 m were linearly interpolated from the surface mapping value to the paravane value. Because the well-mixed upper layer of the ocean was normally deeper than 10 m, the surface mapping and the 10-m paravane readings often were nearly the same (vertical profiler data have shown this assumption to be valid). The product of the processing was an array, with each row representing a 1-m depth and each column representing one paravane undulation. The data array was fed into a contouring package to produce either an isoline contour plot or a false-color vertical map of the ocean.

Sensor Calibrations

All commercially manufactured instruments were calibrated by the respective manufacturer before each cruise. The bathyphotometers were calibrated using a bioluminescent bacterial culture.[11] John Lee of the University of Georgia supplied the freeze-dried organisms to us. The bacteria were dissolved in a culture medium and allowed to grow for about one hour at 32°C. The sample was introduced into the bathyphotometer light chamber, and the sensor output was noted. A 1-mL aliquot of this sample was placed into a National Bureau of Standards traceable laboratory photometer, which measured the sample's light intensity. (The photometer is on loan to APL from the Naval Ocean Research and Development Activity.) The culture was serially diluted to obtain a multipoint calibration.

The transmissometers were calibrated before each deployment by first thoroughly cleaning the window and mirror surfaces and then obtaining in-air and zero transmission readings. The difference between these two readings is equivalent to an in-water value of 85.6% transmission, which is a function of the geometrical and optical surfaces in each transmissometer.

The surface mapping and vertical profiling fluorometers were calibrated with water samples obtained either at the effluent of the surface mapping system or from Niskin bottles. Typically, 1 L of water is vacuum-filtered through a 25-mm-diameter Whatman GF/F glass-fiber filter. The phytoplankton deposited on the filter paper were digested into 90% acetone and fluorometrically analyzed (using the procedures outlined in Strickland and Parsons[12]) with a second fluorometer calibrated before the cruise using purified chlorophyll-*a*. A multivariant regression of chlorophyll and phaeophytin values against fluorometer output was performed to find the calibration coefficients.

The paravane fluorometer was calibrated by periodically obtaining water samples from the surface mapping system when the paravane was at the top of its cycle. Again it was assumed that the water column was homogeneous in the upper 10 to 15 m. To supplement these water samples, additional calibration points were obtained by noting the pigment concentrations determined by the calibrated surface mapping fluorometer at the top of each paravane cycle. A second multivariant regression of all chlorophyll and phaeophytin values against the fluorometer output was performed to find the calibration coefficients.

RESULTS

The principal goals of our field efforts have been to acquire a suitable data set to describe the ocean optical and bioluminescence variability and to determine if there were any physical or biological relationships that might account for the variability. Data from two cruises, August 1986 and March 1988, are presented to illustrate our findings.

Figure 4 shows, for the March 1988 cruise, the false-color contour maps of temperature, chlorophyll-*a* concentration, bioluminescence, and beam attenuation from a north–south tow of about 180 km originating at 35°N 70°W. The tow began at local midnight and continued until noon, with dawn occurring near the 80-km mark. These maps are the results of 201 paravane profiles down to a 90-m depth. The black vertical band at about 125 km, observed in all maps, represents a break in the data caused by changing the nine-track tapes in the data acquisition system. To the right of each map is a color bar keying the colors to a measured quantity.

During the early spring, the mixed layer exceeded 90 m. The temperature map (Fig. 4a) reveals subtle horizontal fluctuations of about 0.2°C. The fluctuations extend from the surface to at least 90 m.

The bioluminescence map (Fig. 4c) also exhibits vertical banding, with the greatest concentration of organisms to either side of the local temperature maximum at about 40 km. Here the night/day transition is pronounced at the 80-km mark, as most bioluminescent organisms either have photoinhibited emissions[13] in daylight or migrate to deeper waters during that time. Another feature commonly observed is that the bioluminescence data are very "noisy." Bioluminescent organisms, particularly in low-productivity waters like the Sargasso Sea, are not found in high concentrations. Typical concentrations may range from several per liter for the small dinoflagellates to less than one per cubic meter for larger zooplankton.

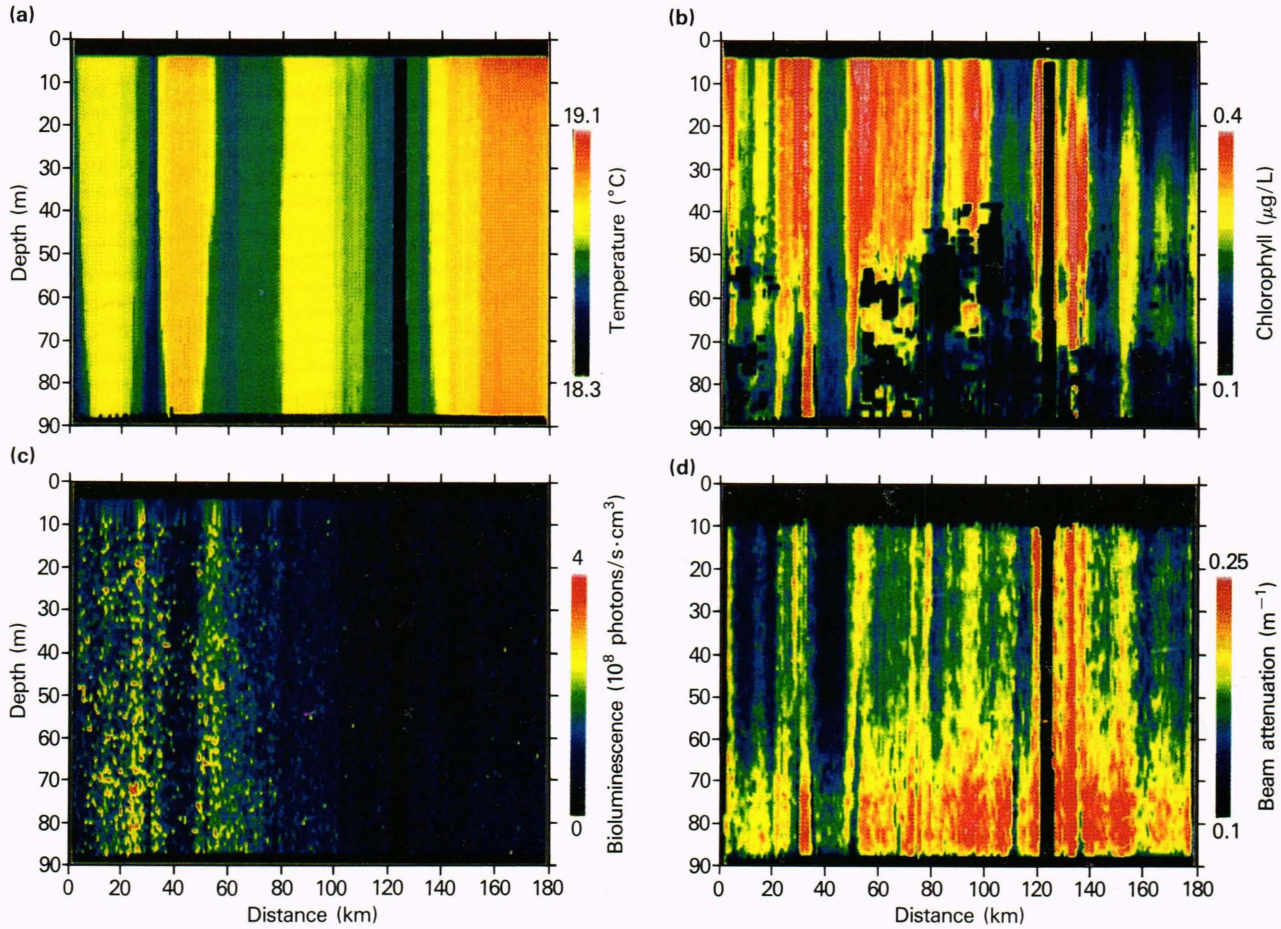

Figure 4—Paravane false-color contour maps of a 180-km north–south tow originating at 35°N 70°W in the Sargasso Sea during the March 1988 cruise: (a) temperature, (b) chlorophyll-*a* concentration, (c) bioluminescence, and (d) beam attenuation.

Bathyphotometers, like the one we use, sample only 1 L/s of water. This small sample volume produces a large amount of scatter in the data. The smearing observed along the top of Fig. 4c is a result of the linear interpolation between the surface mapping and paravane data.

The vertical banding is also obvious in the optical data, represented by the chlorophyll and beam attenuation maps (Figs. 4b and 4d, respectively). The dark patches observed near the center of Fig. 4b result from sensor dropout; for a short time during the middle of the tow, the fluorometer channel would unexplainably go to zero.

The parameters generally exhibit a uniform vertical distribution except that, toward the middle of the tow, chlorophyll showed a decrease below 50 m, while the beam attenuation showed a small increase with depth. Conversely, the horizontal variability would appear patchy if the ocean were viewed from an aircraft or satellite. Figures 5a and 5b show a horizontal cut through the chlorophyll (Fig. 4b) and beam attenuation (Fig. 4d) maps at a depth of 11 m. These traces illustrate the magnitude and extent of the patches and also show a high degree of correlation. To quantify the dominant patch dimensions, we used structure-function calculations.[14] The structure function is the root-mean-square difference of two measurements separated by a distance x'

$$D(x') = \sqrt{2}\ \sigma[1 - R(x')]\ , \qquad (2)$$

where σ is the standard deviation and $R(x')$ is the autocorrelation function. The structure functions for the first 120 km for all parameters are presented in Fig. 6. The first maximum is indicative of half the dominant spatial frequency or the dominant patch size. The first minimum after that peak is the dominant spatial frequency. The separation between the maximum and minimum indicates the significance of these patches. If the time series were a pure sine wave, the structure function would return to zero at the fundamental frequency. As random noise is added to the sine wave, the minimum at the fundamental frequency begins to rise until the noise masks the sine wave. When this happens, the first maximum in the structure function approaches the zero distance, and no discernible minimum is observed. At large separations, the structure function will approach a value equal to $\sqrt{2}\ \sigma$ of the time series.

The temperature structure function (Fig. 6a) indicates a dominant patch size of about 22 km. The chlorophyll, beam attenuation, and bioluminescence structure functions (Figs. 6b, 6c, and 6d, respectively) show a dominant patch size of about 10 to 15 km. The structure functions for each parameter have been calculated at several depths with virtually identical results, indicating that the patches are not surface phenomena, but extend deep into the water column.

As chlorophyll and beam attenuation exhibit similar patch sizes and the two time series displayed in Fig. 5 seem highly correlated, the coherence spectrum of those time series was calculated (Fig. 7). Significant coherence is seen in Fig. 7a at about 7×10^{-5} to 1×10^{-4} m^{-1} (10 to 14 km). The coherence of temperature or bioluminescence with the other parameters (Figs. 7b to 7f) is not significant at any frequency.

Figure 8 presents, for the August 1986 cruise, the false-color contour maps of temperature, chlorophyll-*a*, bioluminescence, and beam attenuation from a northeast tow of about 80 km originating at 34°N 71°W. These maps are from 88 nighttime paravane profiles down to a depth of 90 m. The data are presented on a 180-km abscissa to facilitate comparison with the March 1988 maps. When possible, the color assignments were the same as for the spring data.

We see immediately in Fig. 8 the absence of the vertical banding observed during the spring (Fig. 4). The mixed layer has diminished to a depth of about 20 m, below which we see a pronounced thermocline. The false-color temperature map (Fig. 8a) shows that the mixed layer has

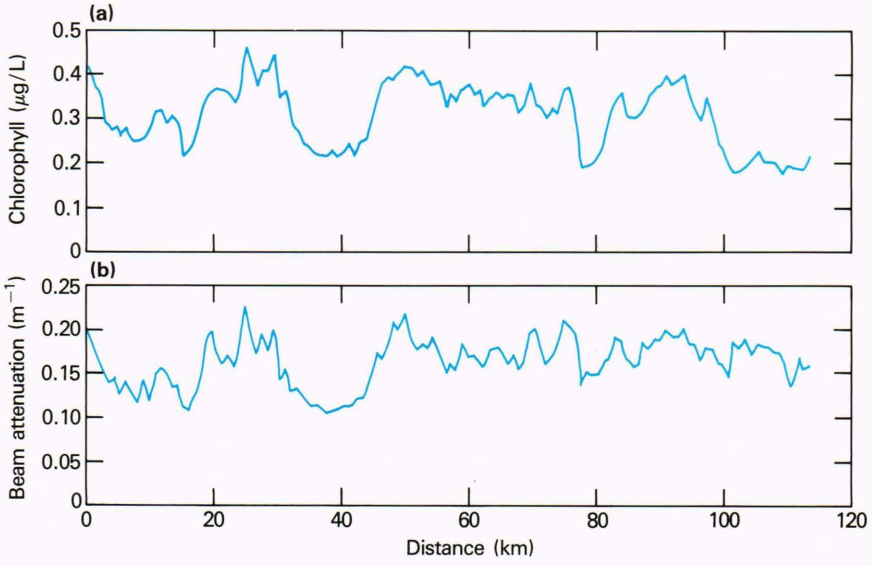

Figure 5—The horizontal trace of (a) chlorophyll-*a* and (b) beam attenuation at an 11-m depth taken from the March 1988 paravane tow.

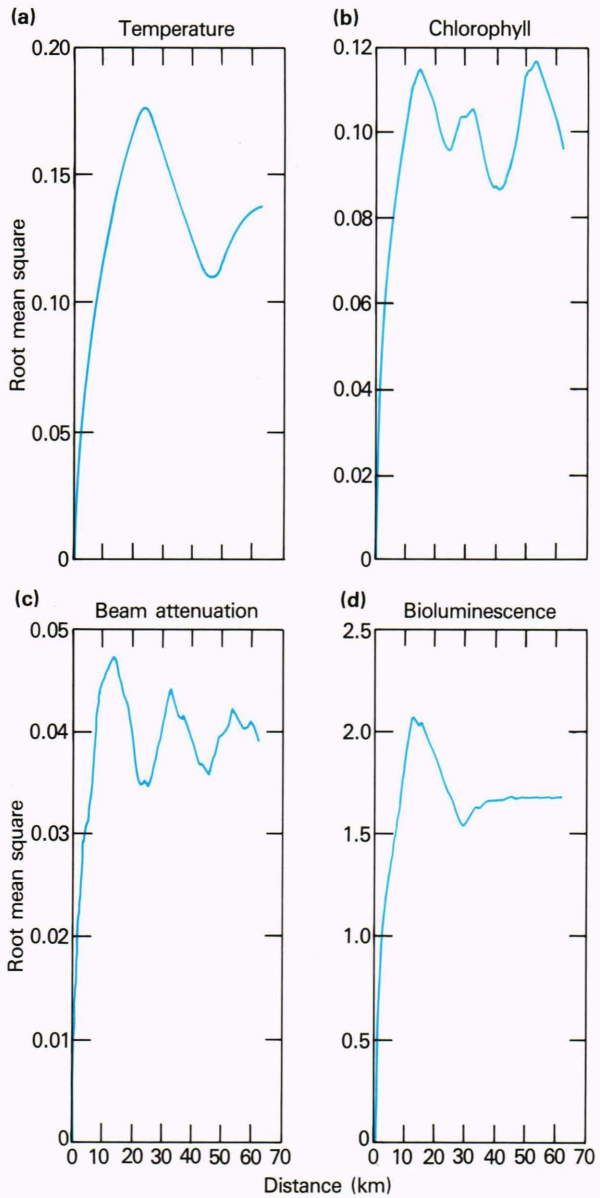

Figure 6—Structure functions of (a) temperature, (b) chlorophyll-*a* concentration, (c) beam attenuation, and (d) bioluminescence at an 11-m depth taken from the March 1988 paravane tow.

a small amount of variability. A horizontal cut through the map at 11 m reveals temperature variations comparable to those observed during the spring.

The chlorophyll map (Fig. 8b) shows very low levels in the upper 60 m of the water column. The upper portion of the deep chlorophyll maximum is observed beginning at about 60 m. The actual depth of the maximum, as determined by the vertical profiler that went to 150 m, was between 90 and 100 m.

The bioluminescence map (Fig. 8c) displays activity of comparable amplitude to the spring, but we see a pronounced subsurface maximum at the base of the mixed layer extending down to about 60 m.

Although the chlorophyll map indicates a very low concentration of phytoplankton in the upper 50 m, the beam attenuation map (Fig. 8d) shows a slight particle maximum in the upper 30 m. This maximum is not intense and is highlighted only because the color table has been adjusted to span the small range of variability observed in the map. Essentially, the vertical structure is uniform, with a small drop-off beginning at about 70 m. Interestingly, the beam attenuation is decreasing at a depth where the chlorophyll is increasing, suggesting that there are fewer particles at depth. But the concentration of chlorophyll per particle is increasing—a commonly observed phenomenon resulting from a physiological adaptation of the phytoplankton crop to the decreased light levels at depth.[15] The environmental agents that determine the standing crop and distribution of particles are not well understood; however, we can reasonably assume that light, nutrient, and advective and turbulent transport fields, as well as the grazing of herbivorous zooplankton, are all important.

Preliminary observations of the maps show little evidence of horizontal patchiness. Figure 9 shows the structure functions at 11 m, where there is little indication of significant length scales.

The coherence spectra for the various parametric combinations (excluding temperature) are shown in Fig. 10. Only chlorophyll and beam attenuation exhibit significant coherence at about 25 km. No significant coherence was observed for temperature.

DISCUSSION

We observed a marked contrast between the optical properties seen during the spring 1988 and summer 1986 tours. In March 1988, high phytoplankton populations and particle concentrations (as shown in the chlorophyll and beam attenuation maps) persist over much of the region and are uniformly distributed over the upper 90 m of the water column. A high degree of horizontal patchiness is also observed, showing roughly a factor of 2 change in the amplitude of the patches. Dominant patch scales have been shown to be about 10 to 15 km, with a high degree of coherence between the phytoplankton population and the particle concentration, suggesting that most particles in the upper water column are viable phytoplankton.

The high degree of coherence observed between chlorophyll and beam attenuation indicates that a simple linear model should describe the relationship. A scatter plot of chlorophyll concentration versus beam attenuation (Fig. 11) indicates that the relationship between these two parameters changes during the course of the tow. The first 70 km of the tow (open squares) produce a very tight linear correlation,

$$\text{beam attenuation} = 0.43\ \text{chlorophyll} + 0.02;$$

$$r = 0.96\ . \qquad (3)$$

Note that the intercept is the beam attenuation coefficient for pure seawater, again suggesting that phytoplankton are primarily responsible for the scattering. The next 50 km (closed circles) show a relaxation and shifting of this relationship,

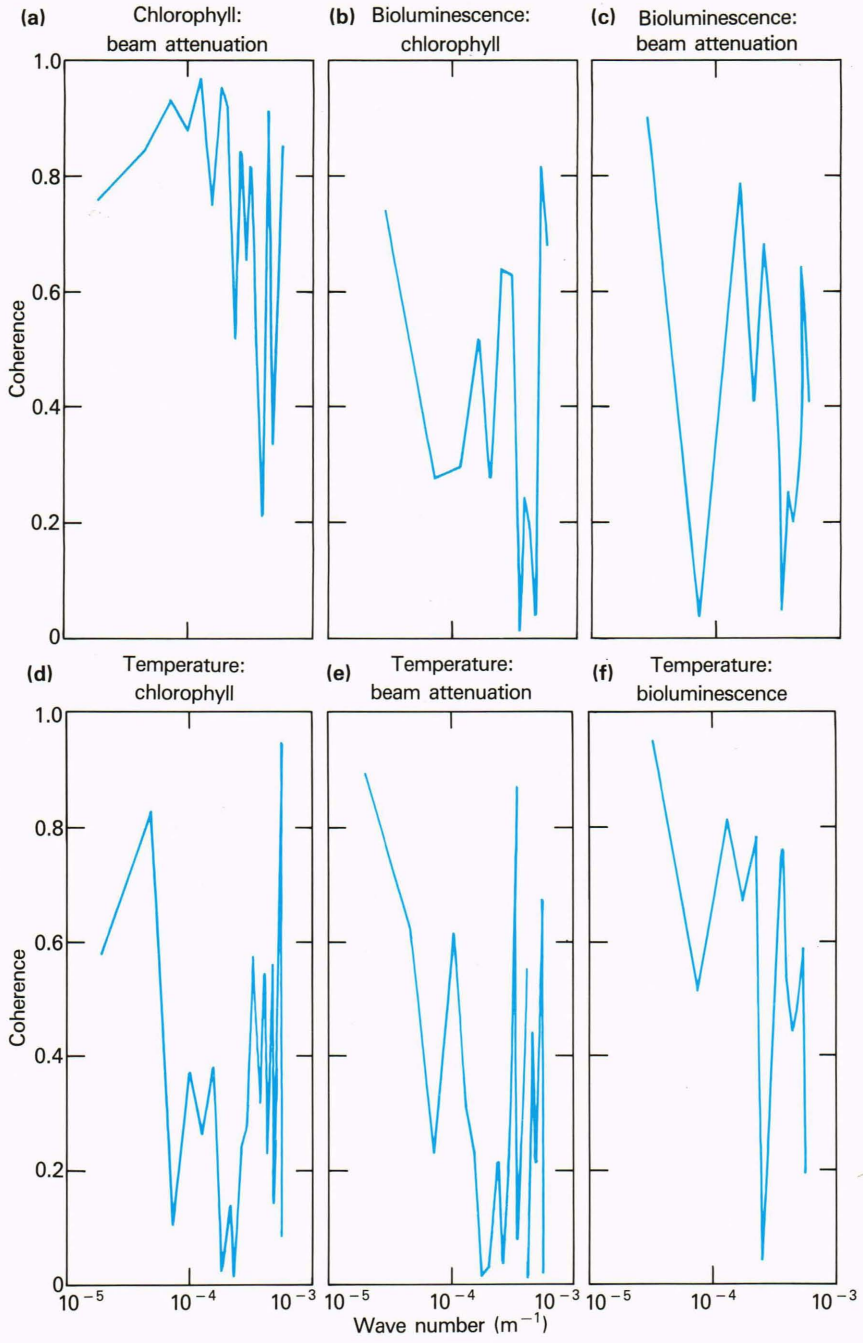

Figure 7—Coherence spectra between combinations of temperature, chlorophyll, beam attenuation, and bioluminescence at an 11-m depth taken from the March 1988 paravane tow.

$$\text{beam attenuation} = 0.184\ \text{chlorophyll} + 0.12; \quad r = 0.80 \ . \tag{4}$$

Here, the intercept is considerably higher. Something other than phytoplankton is contributing to scattering. Perhaps the amount of detritus (nonliving material) has increased. It is unclear what produces the change. Examination of the two time series in Figs. 5a and 5b shows that chlorophyll exhibits a negative low-frequency drift, while the beam attenuation remains nearly constant. One explanation for the different trends may be a false lowering of the chlorophyll levels caused by photoinhibition of the chlorophyll fluorescence during the daytime. The quantum efficiency of chlorophyll fluorescence may be reduced during the daytime because of the channeling of the radiant energy away from fluorescent processes and into photosynthetic processes. No correction has been made to the fluorometer calibration to correct for this possibility. The effect should disappear deeper in the water column, since the radiant flux is attenuated by the water above. Examination of the chlorophyll–beam attenuation relationship at a depth of 35 m shows the same results; therefore, photoinhibition of chlorophyll fluorescence can be ruled out.

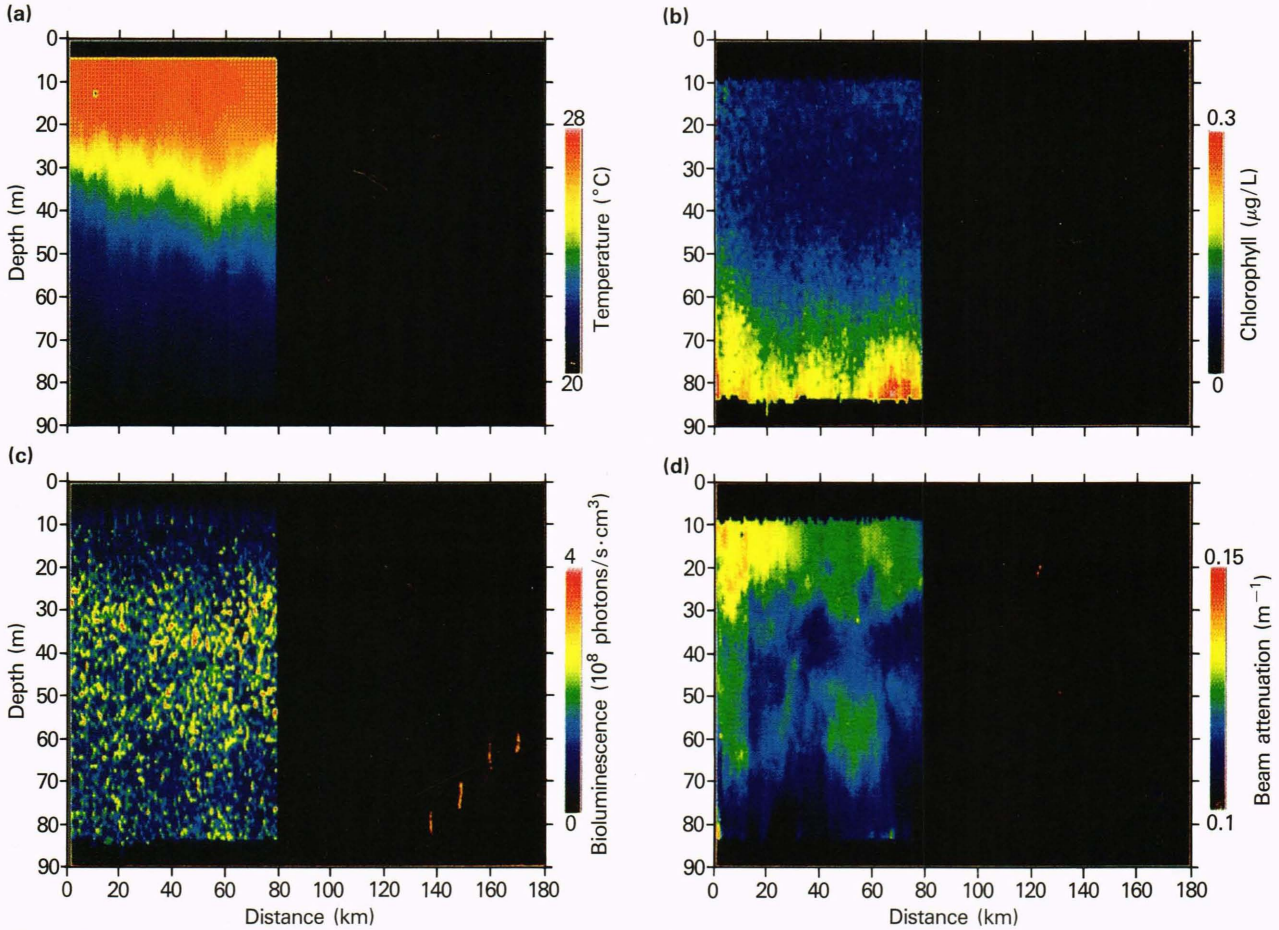

Figure 8—Paravane false-color contour maps of a northeast tow of about 80 km originating at 34°N 71°W in the Sargasso Sea during the August 1986 cruise: (a) temperature, (b) chlorophyll-*a* concentration, (c) bioluminescence, and (d) beam attenuation.

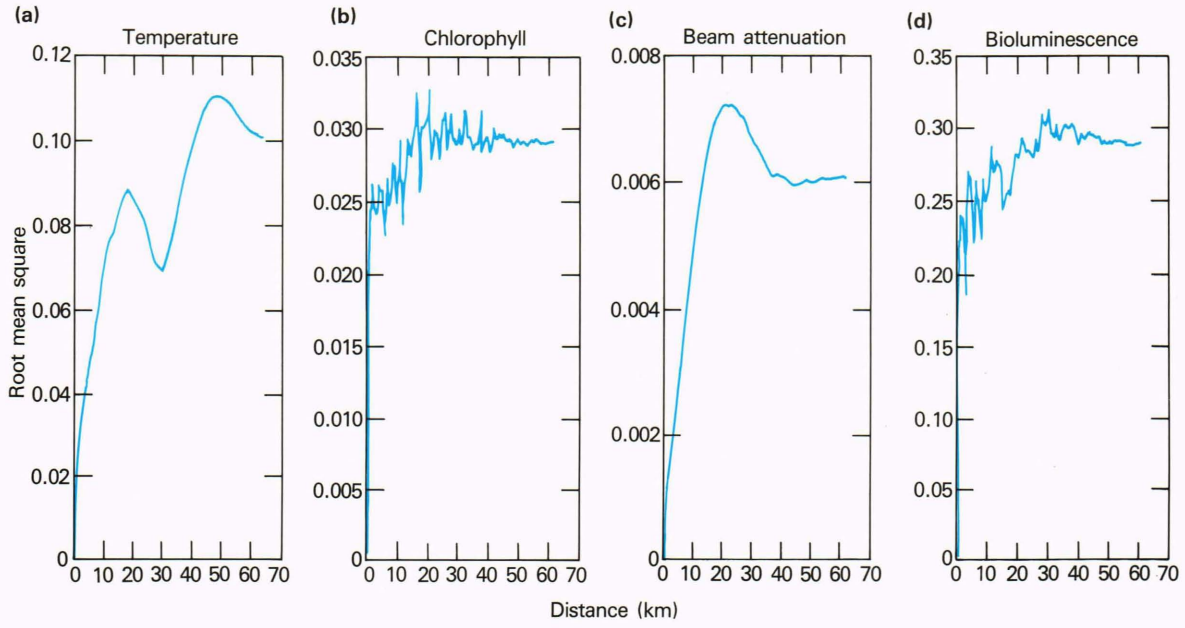

Figure 9—Structure functions of (a) temperature, (b) chlorophyll-*a* concentration, (c) beam attenuation, and (d) bioluminescence at an 11-m depth taken from the August 1986 paravane tow.

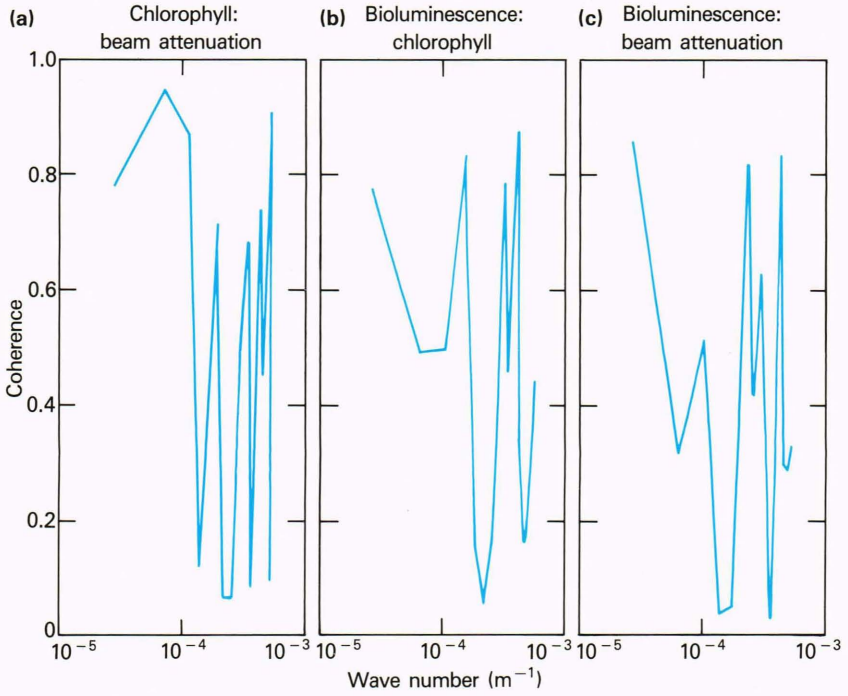

Figure 10—Coherence spectra between combinations of chlorophyll-*a*, beam attenuation, and bioluminescence at an 11-m depth taken from the August 1986 paravane tow.

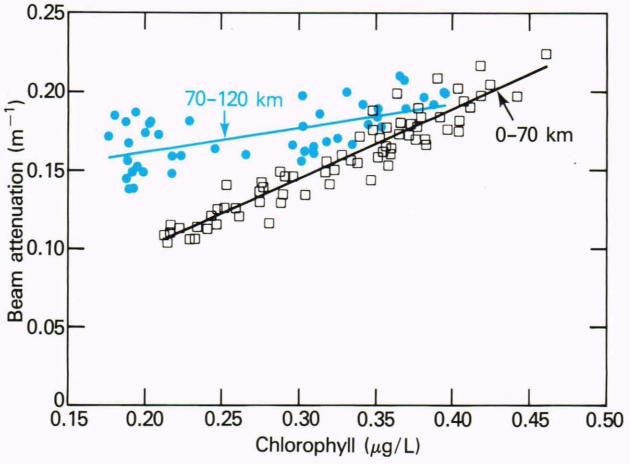

Figure 11—A scatter plot of chlorophyll versus beam attenuation at an 11-m depth taken from the March 1988 paravane tow. Open squares represent the first 70 km of tow; closed circles represent the next 50 km.

The high-plankton standing stock during the spring probably results from high nutrient levels (nitrate levels at the surface were almost 1 μg-atom/L), a stabilization of the water column, and abundant light. During the summer months, the mixed layer becomes shallow, confining the phytoplankton in a high-light region. There, they vigorously produce until the nutrients are nearly depleted, and then the standing stocks virtually disappear. This manifests itself in very low chlorophyll and beam attenuation levels near the surface. Phytoplankton production does continue in the seasonal thermocline, with a deep chlorophyll maximum developing—a classical example of a subsurface feature that cannot be observed in satellite imagery.

A model that predicts the vertical optical structure should incorporate mixed-layer depth, solar flux, and nutrient levels. In the Sargasso Sea, productivity is driven by the combination of nutrient and light levels. During the spring, nutrients are abundant, and production is limited only by available light. A uniform chlorophyll distribution should result down to the euphotic depth (1% light level). During the summer, there is ample light for production but little "food." At the depth where there are sufficient nutrients and light, a chlorophyll maximum forms. Below that depth, there is insufficient light to support growth. We are currently developing a model that incorporates these features.

The patchiness observed during the spring is probably created by either physical (wind stress, localized upwelling or downwelling, etc.) or biological (growth and predation) processes. A clue to the source of the patchiness may be obtained by computing the variance spectra of the variables.[16] The relative relationship between the variance of bioluminescence, chlorophyll, or beam attenuation and temperature may help determine whether the patches are controlled by biological or physical processes. The power spectra for the variables at a depth of 11 m for both seasons are shown in Fig. 12. We assumed that since the distribution of temperature variance is determined by physical processes, then similar spectral shapes for bioluminescence, chlorophyll, and beam attenuation would suggest that their spatial distributions are also driven by physical processes.[17] During the spring, the slopes of all the spectra are between 2 and 3, indicating that physical forcing dominates. But the bio-optical spectra during the summer are virtually flat, indicating that localized growth and predation dominate the variability.

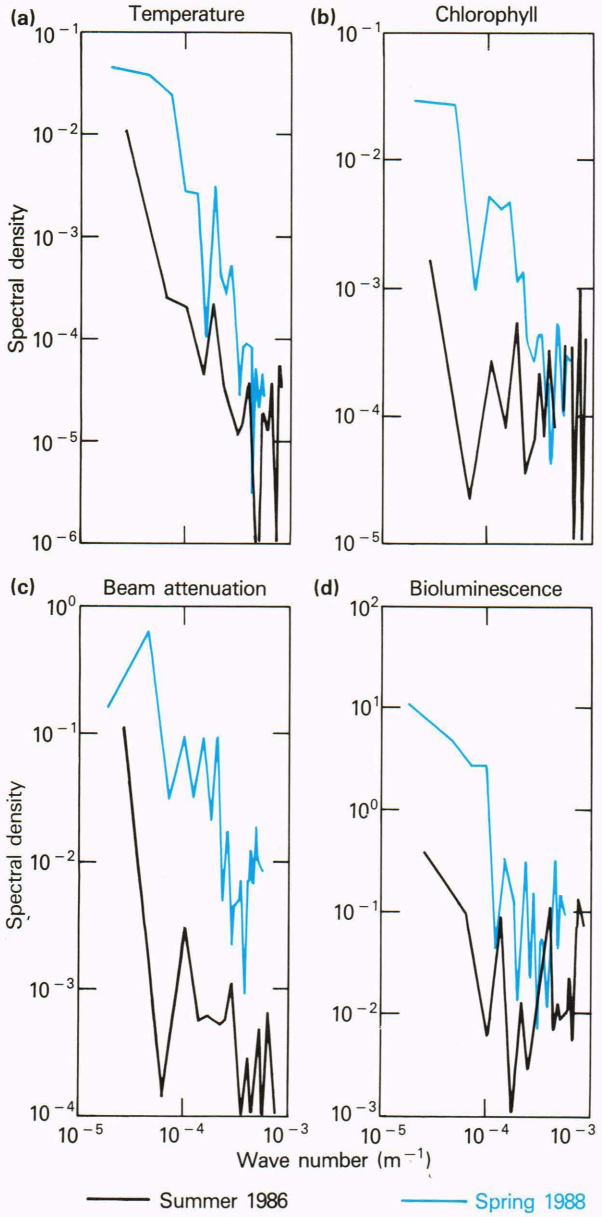

Figure 12—Spectral density estimates of (a) temperature, (b) chlorophyll-*a*, (c) beam attenuation, and (d) bioluminescence at an 11-m depth taken from the March 1988 and August 1986 paravane tows.

SUMMARY

We have briefly described in this article the environmental sampling system developed by APL and some results obtained from two cruises in the northern Sargasso Sea. Preliminary analysis of the data revealed the following:

1. Phytoplankton production in the upper 90 m of the water column is markedly higher in the spring than in the summer, causing a corresponding decrease in water transparency.

2. During the spring, the vertical structure of the water column shows remarkable uniformity, while the horizontal structure shows great variability. The dominant length scale for the bio-optical properties in the spring was about 10 to 14 km. No dominant length scale was observed in the summer data.

3. A strong coherence between chlorophyll and beam attenuation in the spring was determined for length scales greater than 5 km. No coherence is observed between bioluminescence and any other parameter.

4. During the summer, the upper 50 to 60 m of the water column are relatively devoid of phytoplankton, but at about 100 m, a deep chlorophyll maximum exists. The particle distribution is relatively uniform in the water column, suggesting that the chlorophyll maximum is not an increase in the phytoplankton standing stock, but rather an increase in the amount of chlorophyll per cell.

REFERENCES

[1] W. A. Hovis, D. K. Clark, F. Anderson, R. W. Austin, W. H. Wilson, E. T. Baker, D. Ball, H. R. Gordon, J. L. Mueller, S. Y. El Sayed, B. Sturm, R. C. Rigley, and C. S. Yentsch, "Nimbus 7 Coastal Zone Color Scanner: System Description and Initial Imagery," *Science* **210**, 60–63 (1980).

[2] R. C. Smith, K. S. Baker, and R. W. Eppley, "Correlation of Primary Production as Measured Aboard Ship in Southern California Coastal Waters and as Estimated from Satellite Chlorophyll Images," *Mar. Biol.* **66**, 281–286 (1982).

[3] H. R. Gordon, D. K. Clark, J. L. Mueller, and W. A. Hovis, "Phytoplankton Pigments from the Nimbus 7 Coastal Zone Color Scanner: Comparison with Surface Measurements," *Science* **210**, 63–66 (1980).

[4] R. W. Austin and T. J. Petzold, "The Determination of the Diffuse Attenuation Coefficient of Sea Water Using the Coastal Zone Color Scanner," in *Oceanography from Space*, J. F. R. Gower, ed., Plenum Press, New York, pp. 239–259 (1981).

[5] J. T. McMurtrie, Jr., *Spatial Structures of Optical Parameters in the California Current as Measured with the Nimbus 7 Coastal Zone Color Scanner*, master's thesis, Naval Postgraduate School, Monterey, Calif. (1984).

[6] N. G. Jerlov, *Marine Optics*, Elsevier Scientific Publishing, Amsterdam (1976).

[7] J. L. Mueller, *The Influence of Phytoplankton on Ocean Color Spectra*, doctoral thesis, Oregon State University, Corvallis (1973).

[8] K. S. Baker and R. C. Smith, "Bio-Optical Classification and Model of Natural Waters. 2," *Limnol. Oceanogr.* **27**, 500–509 (1982).

[9] H. R. Gordon and A. Y. Morel, *Remote Assessment of Ocean Color for Interpretation of Satellite Visible Imagery*, Springer-Verlag, New York (1983).

[10] C. V. Nelson, *Bio-Optical Measurement Platforms and Sensors*, JHU/APL STD-R-1160 (1985).

[11] I. B. C. Matheson, J. Lee, and E. F. Zalewski, "A Calibration Technique for Photometers," *SPIE* **489**, *Ocean Optics VII*, 380–383 (1984).

[12] J. D. H. Strickland and T. R. Parsons, *A Practical Handbook of Seawater Analysis*, Bulletin 167, Fisheries Research Board of Canada (1972).

[13] E. Swift and V. Meunier, "Effects of Light Intensity on Division Rate, Stimulable Bioluminescence and Cell Size of the Oceanic Dinoflagellates *Dissodinium Lunula, Pyrocystis Fusiformis* and *P. Noctiluca*," *J. Phycology* **12**, 14–22 (1976).

[14] R. F. Gasparovic, *Effects of Spatial Variability on Remotely Sensed Sea-Surface Temperature*, JHU/APL STD-R-822 (1983).

[15] D. A. Kiefer, "Microplankton and Optical Variability in the Sea: Fundamental Relationships," in *Proc. Ocean Optics IV*, p. 489 (1984).

[16] J. S. Bendat and A. G. Piersol, *Random Data: Analysis and Measurement Procedures*, Wiley-Interscience, New York (1971).

[17] K. I. Denman, "Covariability of Chlorophyll and Temperature in the Sea," *Deep Sea Res.* **23**, 539–550 (1976).

ACKNOWLEDGMENTS—The author wishes to acknowledge the outstanding efforts of W. E. Sparrow, J. T. Velky, and K. E. Grempler, without whom these data could not have been collected.

THE AUTHOR

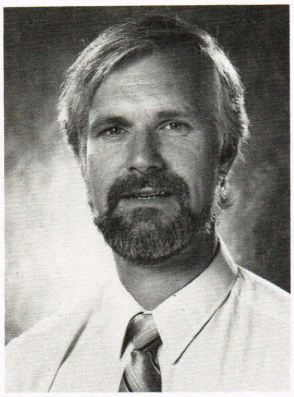

DANIEL G. ONDERCIN was born in Cleveland in 1951. He received a B.S. degree in chemistry from Ohio University (1973) and a Ph.D. degree in physical chemistry from the University of Rochester (1978). Dr. Ondercin joined APL in 1978 as a member of the Environmental Group in the Submarine Technology Department. His activities have included trace metal analysis of seawater and methane gas recovery in landfills. He has been involved in planning and conducting open-ocean experiments in marine bioluminescence and optics since 1983.